Phys. Status Solidi C **11**, No. 11–12, 1697–1702 (2014) / **DOI** 10.1002/pssc.201400036

physica status solidi c
www.pss-c.com
current topics in solid state physics

Influence of copper contamination on the illuminated forward and dark reverse current-voltage characteristics of multicrystalline p-type silicon solar cells

Tleuzhan Turmagambetov, Sébastien Dubois*, Jean-Paul Garandet, Benoit Martel, Nicolas Enjalbert, Jordi Veirman, and Etienne Pihan

CEA, LITEN, INES, 50 Avenue du Lac Léman, 73377 Le Bourget du Lac, France

Received 28 April 2014, accepted 18 May 2014
Published online 11 September 2014

Keywords multicrystalline silicon, solar cells, copper, gettering, hydrogenation

* Corresponding author: e-mail sebastien.dubois@cea.fr, Phone: +33 (0)4 79 79 29 12, Fax: +33 (0)4 79 68 80 49

We studied the influence of copper (Cu) on the performances of conventional photovoltaic (PV) solar cells by growing two multicrystalline (mc) boron-doped silicon (Si) ingots from ultra-pure feedstocks, one of these feedstocks being deliberately contaminated with 90 ppm wt of Cu. Industrial-like solar cells were fabricated and the associated external gettering and hydrogenation effects were studied. An originality of our approach consisted in evaluating the forward but also reverse current-voltage (I-V) characteristics of the fabricated cells. Furthermore we assessed the stability under illumination of the PV parameters as Cu is known to be responsible for light-induced degradations (LID) of the carrier lifetime. On the one hand we unexpectedly showed that the PV conversion efficiency (η) was not affected by the initially large Cu concentrations. We demonstrated that it was due to the complementary actions of the external gettering effect developed by the phosphorus-diffusion and the bulk hydrogenation. The Cu-addition slightly enhanced the pn junction hard breakdown, however the extracted junction breakdown voltages fulfilled the common industrial requirements for this parameter. On the other hand we highlighted significant decreases under illumination of the PV performances for the Cu-contaminated solar cells fabricated from wafers coming from the upper part of the ingot (i.e., samples with the highest Cu concentration). These decreases could be explained by the previously proposed mechanisms in the literature, which argue that the excess charge carriers could reduce the electrostatic repulsion between interstitial Cu ions and Cu precipitates, this effect enhancing the Cu precipitation.

1 Introduction Copper (Cu) is a common element in Solar-Grade (SoG) silicon (Si). Owing to a large diffusion coefficient Cu contamination may easily occur during Si PV solar sell manufacturing [1]. In addition Cu is used as a catalyst for the production of fluidized bed reactor polysilicon. Eventually the replacement of expensive screen-printed silver front contacts with Cu-plated contacts might further increase the probability of Cu contamination. Consequently studies about the properties of Cu-contaminated Si solar cells are of paramount importance. Recently, Coletti et al. [2] conducted high level studies about the influence of Cu by growing multicrystalline (mc) Si ingots deliberately contaminated by this element (about 100 ppm wt of Cu were added in the feedstock). Solar cells were fabricated and one of the main results of this pioneering work was that the Cu-addition affected both the base carrier lifetime and the electrical quality of the phosphorus (P)-diffused layer. The goal of our study was to reproduce this study, but using an improved solar cell fabrication process compatible with PV conversion efficiencies (η) as high as 17% with mc wafers. We also used specific experimental protocols in order to highlight the efficiency of the external gettering and bulk hydrogenation steps, associated with a conventional solar cell process. Furthermore, we developed a complementary and original approach via the evaluation of the forward but also reverse current-voltage (I-V) characteristics of the fabricated cells. Finally, we assessed the stability under illumination of the PV parameters as Cu

is known to be responsible for light-induced degradations (LID) of the carrier lifetime [3].

2 Experimental details

For this study, two mc Si ingots were grown by directional solidification from ultra-pure electronic-grade Si (EG-Si). Both ingots were boron (B)-doped in order to obtain p-type Si wafers with standard resistivity (ρ), around 1 Ωcm. The first ingot (mc-Ref) was grown without intentional contamination. The feedstock used for the second ingot (mc-Cu) was deliberately contaminated with 90 ppm wt, or equivalently 2×10^{18} cm^{-3}, of Cu.

On vertical cuts from both ingots, the interstitial oxygen (O_i) concentration ([O_i]) and the substitutional carbon (C_s) concentration ([C_s]) were measured by Fourier Transform Infrared Spectroscopy (FTIR) along the ingot's height (calibration coefficient of 3.14×10^{17} cm^{-2}). The Cu concentrations ([Cu]) were determined by Glow Discharge Mass Spectroscopy (GDMS) analyses. This technique gives for a given impurity its total concentration, irrespective of its chemical state (dissolved, precipitated, ionized/neutral) within the Si bulk. The uncertainties associated with the GDMS analyses were given to be about 20%. The experimental [O_i], [C_s] and [Cu] variations along the height of both ingots are shown in Fig. 1. The experimental [Cu] are also compared with the expected [Cu], calculated from Scheil's law, using for the segregation coefficient (k) the value given in [4] ($k = 4\times10^{-4}$).

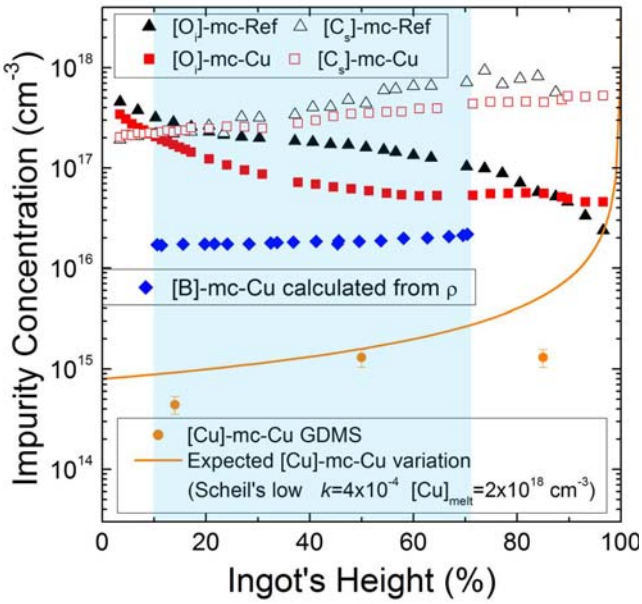

Figure 1 [O_i], [C_s], [B] and [Cu] variations along the ingot's height. The coloured area shows the ingot's fraction which was used for the solar cell fabrication.

Both ingots were cut in square wafers (area 156×156 mm^2) with a thickness of about 200 µm. Some wafers were collected at regular intervals along the ingot's height and the ρ were measured using a four-point probe setup and averaged over 25 positions across the wafer surface. From the experimental ρ, the B concentrations ([B]) were calculated using Arora's model for the computation of the hole mobility [5]. The [B] variation along the ingot's height is shown in Fig. 1.

Around 15 wafers were sampled at regular intervals along the ingots' height and transformed into solar cells following an industrial process. Both surfaces were texturized by the anisotropic chemical attack developed by the KOH solution. The n^+ emitter was formed by phosphorus (P) diffusion. Then a hydrogenated Si nitride (SiN_x:H) layer used as antireflection coating was deposited on the front surface by plasma-enhanced chemical vapour deposition. The silver front and aluminium rear electrodes were deposited by screen printing before rapid annealing. Junction opening was performed by laser cutting. The fabricated solar cells were characterized by illuminated forward and dark reverse I-V measurements. For the forward I-V measurements standard illumination and temperature were used (AM1.5G; 0.1 Wcm^{-2}; 25 °C). Notice that these measurements were performed without prior illumination. From these measurements the short-circuit current density (J_{sc}), the open-circuit voltage (V_{oc}), the fill factor (FF) and the η were extracted. Furthermore voltage-resolved reverse bias electroluminescence (ReBEL) measurements were performed at room T on the full cell to image the regions related to breakdown sites. Electroluminescence analyses were also acquired in forward polarization. The grain boundary (GB) distribution was in parallel imaged by high-resolution reflectance measurements (on KOH textured wafers).

Cells fabricated from wafers from the bottom and top parts of the ingots were then placed on a hot plate under a 0.5 Sun illumination at 60 °C and the V_{OC} was monitored in order to evidence possible LID effects. When the V_{OC} presented stable values, the illumination was stopped. The LID amplitudes for all I-V parameters were extracted from I-V measurements before/after the prolonged illumination.

In order to investigate the external gettering effect developed by the P-diffusion, for both ingots, as-received and P-diffused twin wafers experienced additional chemical polishing (particularly to etch the diffused emitter), and both surfaces were electrically passivated by SiN_x:H layers. Then the effective carrier lifetime (τ_{eff}) was mapped via the micro-wave photoconductance decay technique (µW-PCD).

The hydrogenation effects were evaluated by fabricating solar cells from twin wafers, with and without the SiN_x;H layer, source of hydrogen (H). Then light beam induced current (LBIC) mappings were performed at various near infrared wavelengths (spatial resolution 125 µm), from which were calculated the effective electron diffusion length (L_{eff}).

3 Results and discussion

3.1 Compositional properties We can notice (Fig. 1) that [C_s] and [O_i] were slightly higher for mc-Ref than for mc-Cu. Similar crucibles and coatings were used for the solidification of both ingots. However, the ingots were grown in different furnaces with various time-temperature profiles, which could contribute to the small highlighted differences for [C_s] and [O_i]. Regarding the [Cu], the experimental values are slightly lower than the expected data. Furthermore, the experimental [Cu] did not significantly vary along the ingot's height (particularly between the middle and the top part of the ingot). This could be related to Cu evaporation from the melt and to the high Cu diffusivity in solid Si. Indeed during the ingot cooling, Cu is able to diffuse on few centimetres, which would contribute to the homogenization of the [Cu].

3.2 Illuminated forward I-V characteristics Figure 2 presents the FF and the η of the reference and Cu-contaminated solar cells, as a function of the initial location of the wafers along the ingot's height. Firstly we can notice that for both ingots, the FF values, mainly governed by the quality of the solar cell fabrication process (e.g., emitter and metallization), were higher than 79.5%. This means that no major issues were met with the cell fabrication process and consequently relevant comparisons can be made between the reference and the Cu-contaminated samples.

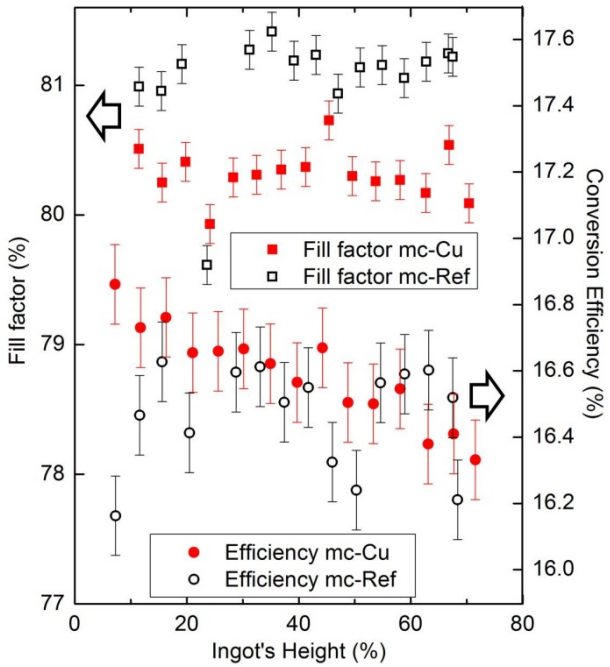

Figure 2 Variations of FF and η of the fabricated solar cells along the ingot's height.

Unexpectedly, in contradiction with the results presented in [2], the introduction of large [Cu] in the feedstock did not affect the η. The average η for the reference and the Cu-contaminated solar cells were equal to 16.5% and 16.6%, respectively. The best measured η, around 16.9%, were even obtained for the Cu-contaminated cells, despite the KOH texturation step, giving high average reflectances with mc samples.

Figure 3 presents the V_{oc} and the J_{sc} of the reference and Cu-contaminated solar cells, as a function of the location of the wafers along the ingot's height. In good agreement with the fact that the η was not affected by the Cu-contamination, similar V_{oc} were extracted for both the reference and the Cu-contaminated solar cells.

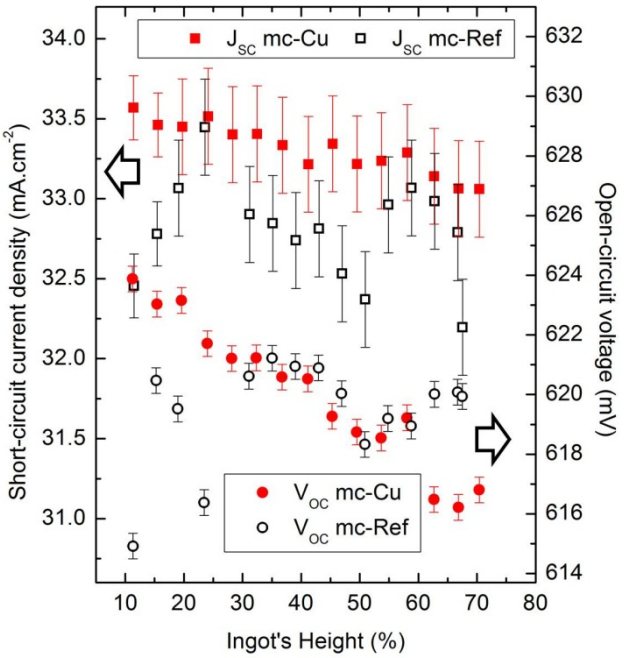

Figure 3 Variations of J_{sc} and V_{oc} of the fabricated solar cells along the ingot's height.

Regarding the J_{sc} values, they are slightly higher for the Cu-contaminated cells. As will be shown later on, such an improvement is also observed on the τ_{eff} mappings. Such unexpected results which should be confirmed by other and complementary measurements are not fully understood. Mechanisms such as the direct electrical passivation of dislocations by Cu atoms as reported in [6], or the presence of liquid Cu silicides during the cooling of the ingot which would develop internal gettering effects as reported in [7], could contribute to these weak effects.

3.3 Dark forward I-V characteristics This part focuses on the influence of the Cu contamination on the absolute value of the hard breakdown voltage (V_{bd}) of Si solar cells. Hard breakdown refers to the ultimate breakdown mechanism, triggered by avalanche multiplication. V_{bd} is a key parameter that governs the long-term performances of PV modules. When a solar cell in a module is shaded, it

can be reverse biased and act as a receptor thereby severely limiting the module output power. Additionally if the reverse bias is close to V_{bd}, large currents can flow locally through the cell leading to thermal damage. To mitigate these effects by-pass diodes are usually implemented. However they are only efficient in standard modules provided that V_{bd} is higher than around 12 V. The breakdown voltage can be degraded by the presence of metallic impurities, especially when they are in the form of precipitates in the space charge region of the p-n junction.

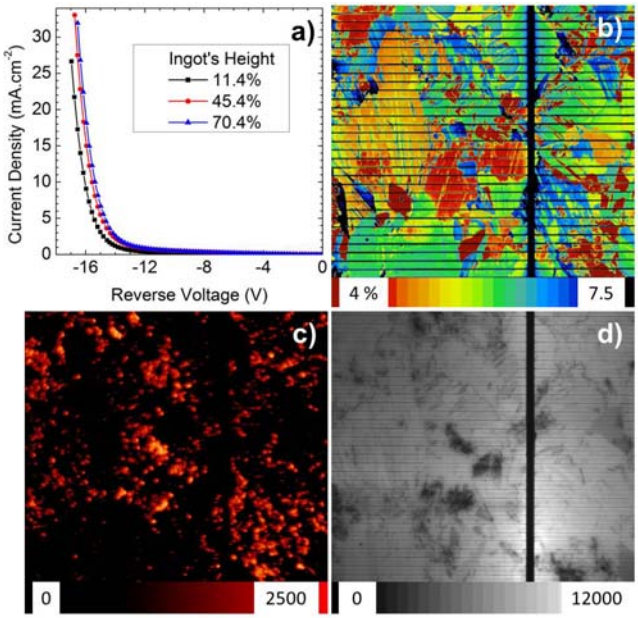

Figure 4 (a) Dark reverse I-V measurements of Cu-contaminated solar cells fabricated from wafers initially located in the top, middle and bottom parts of the ingot. (b) Reflectance mapping (unit in %) obtained with an incident monochromatic light with a wavelength equal to 946 nm; (c) reverse and (d) and forward EL images (arbitrary units) of a solar cell fabricated from a wafer initially located in the middle part of the ingot.

The dark reverse I-V measurements of three Cu-contaminated solar cells, fabricated from wafers initially located in the bottom, middle and top parts of the ingot are shown in Fig. 4a. The main result is that these cells featured absolute V_{bd} values higher than 12 V. Therefore solar cells fabricated from highly Cu-contaminated mc wafers, can fulfil the industrial requirements for the V_{bd}.

However, we can notice that the higher the [Cu], the lower the absolute V_{bd}. Thus Cu would have a slight influence on the p-n junction hard breakdown, even if the effect of the weak increase of the majority charge carrier density on the breakdown cannot totally be ruled out. This could be due to the presence of Cu precipitates located across the p-n junction [8], however, further analyses should be conducted to validate this hypothesis.

It is particularly interesting to compare the ReBEL analysis (Fig. 4c), which can be seen as an image of the breakdown sites, with the reflectance mapping (Fig. 4b), which is representative of the grain structure, and the forward electroluminescence analysis (Fig. 4d). We can notice that the junction breakdown mainly occurs along some grain boundaries and within regions rich in clusters of crystallographic defects, probably dislocations. As such defects could enhance the Cu precipitation it could reinforce the previous mentioned hypothesis (enhancement of the breakdown by the Cu precipitates). However, other mechanisms, independent of the Cu contamination, as an improved P diffusion along dislocations which would modify the morphology of the p-n junction and enhance the breakdown [9] cannot totally be ruled out.

3.4 Effects of the P-diffusion τ_{eff} was measured on as-received and P-diffused twin wafers. The ratio (r_P) between the τ_{eff} measured on the P-diffused samples (τ_{diff}) and the as-received wafers (τ_{init}) was then computed and mapped. The obtained τ_{init}, τ_{diff} and r_P mappings, for reference and Cu-contaminated samples initially located in the middle part of the ingots, are shown in Fig. 5 and Fig. 6, respectively.

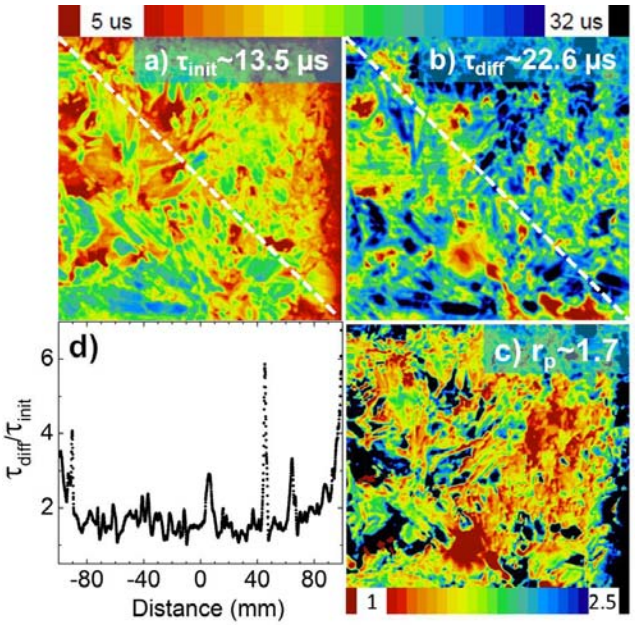

Figure 5 τ_{eff} mapping obtained on as-received (a) and P-diffused (b) twin wafers from the mc-Ref ingot (52% of the ingot's height). (c) Mapping of the ratio (r_P) between the τ_{eff} measured on the P-diffused samples (τ_{diff}) and the as-received wafers (τ_{init}). (d) r_P variation along the white line shown in (a) and (b).

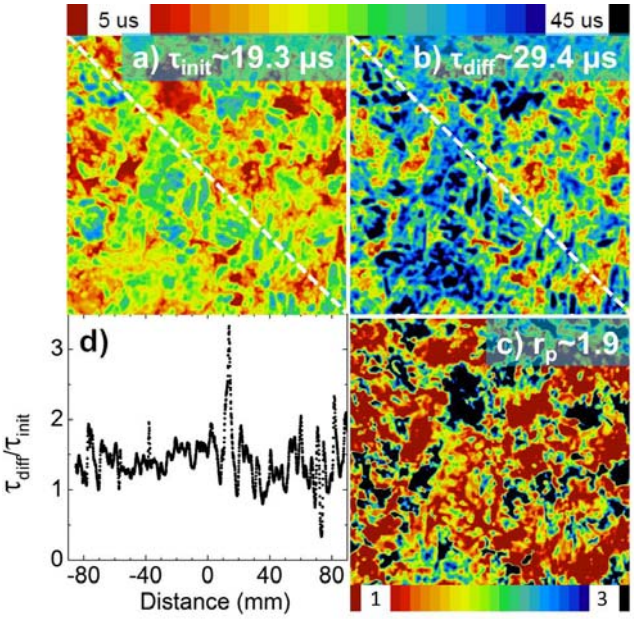

Figure 6 τ_{eff} mapping obtained on as-received (a) and P-diffused (b) twin wafers from the mc-Cu ingot (52% of the ingot's height). (c) Mapping of the ratio (r_P) between the τ_{eff} measured on the P-diffused samples (τ_{diff}) and the as-received wafers (τ_{init}). (d) r_P variation along the white line shown in (a) and (b).

For both, the reference samples and the Cu-contaminated samples, τ_{eff} values were significantly improved by the P-diffusion, since they were multiplied by about 2. This is consistent with the view that fast diffusers, can be efficiently removed from the bulk via the external gettering effect developed by the P-diffusion. For the Cu-contaminated samples, assuming that the initial carrier lifetime was governed by recombination throughout Cu-related defects (isolated atoms or precipitates), this result was expected, since during the P-diffusion step, Cu can migrate on lengths significantly higher than the thickness of the wafer. For the reference wafer, as an improvement of the carrier lifetime by the P-diffusion step was also observed, other fast diffusers (e.g., Fe [10]) could be involved.

3.5 Effects of bulk hydrogenation Figure 7 presents the L_{eff} values determined on Cu-contaminated solar cells fabricated from twin wafers, with (Fig. 7a) and without (Fig. 7b) the presence of a SiN_x:H layer. The ratio (r_H) between the L_{eff} measured on the cell with the SiN_x:H layer and the L_{eff} measured on the cell without the SiN_x:H layer was then computed and mapped. In parallel, is shown a reflectance mapping, revealing the grain structures of the studied samples.

We can notice that the bulk hydrogenation improved the overall bulk electrical properties since the average L_{eff} was multiplied by about 1.2 via the presence of the SiN_x:H layer. On the one hand, the presence of an H source significantly enhanced the quality of the grain boundaries and the regions where dislocations clustered during the crystallisation stage. This could be particularly due to the electrical passivation by H of the dangling bonds. On the other hand, interestingly, within the poorly dislocated grains, the introduction of H atoms slightly degraded L_{eff}. This result is not fully understood but could be due to the formation of H-Cu complexes, which are known for introducing recombinant energy levels in the Si band gap [11].

As the dislocation-rich region are usually regions poorly sensitive to the main external gettering technologies, it confirms, as previously demonstrated [10], that the P-diffusion step and the bulk hydrogenation have complementary actions, which improve the overall Si bulk properties when the material is initially highly contaminated by fast diffusing metal impurities.

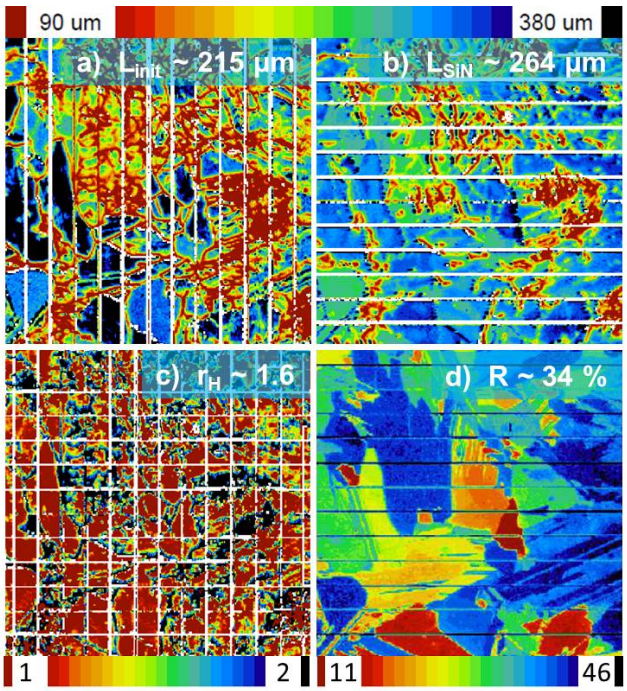

Figure 7 L_{eff} mapping obtained on Cu-contaminated solar cells with (a) and without (b) the SiN_x:H layer (wafers from the middle part of the ingot). (c) Mapping of the ratio (r_H) between the L_{eff} measured on the samples with and without the SiN_x:H layer. (d) Reflectance mapping (unit in %) obtained with an incident monochromatic light with a wavelength equal to 406 nm.

3.6 Effects of prolonged illuminations Studies focused on the evolution of the η under illumination are very important for solar cells fabricated from p-type B-doped Si [12]. Indeed, with such substrates, LID mechanisms can occur, due to the formation (or activation) of boron-oxygen related complexes which act as virulent charge carrier recombination centers and degrade η. In mc-Si with standard [B], the LID effects due to the B-O related complexes usually occur for [O_i] higher than 2-3×10^{17} cm^{-3} and therefore mainly affect the wafers from the bottom part of the ingots, where [O_i] are the highest.

Figure 8 presents the relative η losses evaluated after complete LID following prolonged illumination (~65 hours). For the solar cells fabricated using wafers initially located in the bottom part of the ingot, the η losses were in good agreement with the values usually obtained studying mc wafers from this part of the ingot. The losses were markedly higher for the reference cell, in good agreement with the higher [O_i], revealed by the FTIR analyses.

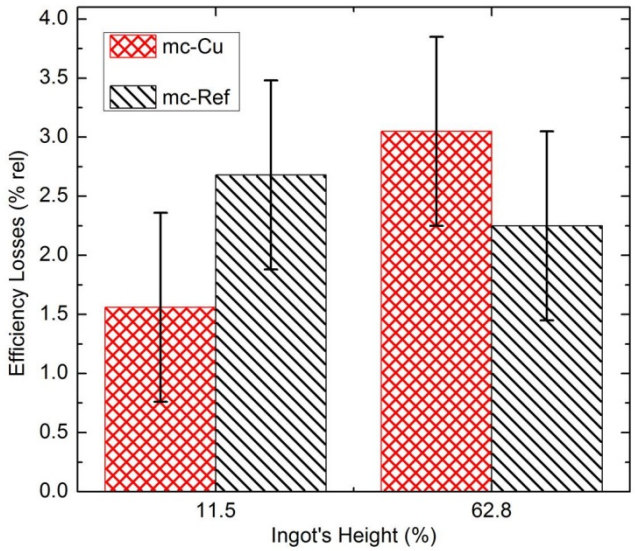

Figure 8 mc-Cu and mc-Ref solar cells relative efficiency losses evaluated after a prolonged illumination.

Unexpectedly, the solar cells fabricated from wafers initially located in the upper part of the ingot, featured significant η losses. As the [O_i] in this part of the ingot are the lowest, it probably means that the B-O complexes are not responsible for these high losses. Interestingly it is known in the literature that Cu can be responsible for LID [3, 13-15] even present at low concentration ([Cu] ~ 10^{13} cm^{-3}). As the evaluated losses are higher for the Cu-contaminated cell, it probably means that Cu is a key contributor to the observed LID. According to the previous studies of the literature (e.g., [3]), under illumination the excess charge carriers would reduce the electrostatic repulsion between positively charged interstitial Cu ions (non-recombinant) and negatively charged Cu precipitates (highly recombinant), this effect enhancing the Cu precipitation. In order to bring further insights into these degradation mechanisms in mc samples, we are now conducting studies at the Si wafer level, via carrier lifetime measurements under prolonged illumination.

4 Conclusion We studied the influence of Cu contamination on the performances of industrial-like solar cells by growing two mc B-doped silicon (Si) ingots from ultra-pure feedstocks, one of these feedstocks being deliberately contaminated with 90 ppm wt of Cu. We unexpectedly showed that the η was not affected by the initially large [Cu]. We demonstrated that it was due to the complementary actions of the external gettering effect developed by the P-diffusion and the bulk hydrogenation. The Cu-addition slightly degraded the pn junction hard breakdown, however, the extracted V_{bd} fulfilled the common industrial requirements for this parameter. We evidenced significant decreases under illumination of the PV performances for the Cu-contaminated solar cells fabricated from wafers coming from the upper part of the ingot (i.e., samples with the lowest [O_i] and the highest [Cu]). These decreases could be explained by the previously proposed mechanisms in the literature, which argue that under illumination the excess charge carriers could reduce the electrostatic repulsion between interstitial Cu ions and Cu precipitates, this effect enhancing the Cu precipitation.

References

[1] K. Graff, Metal Impurities in Silicon-Device Fabrication, 2nd edn. (Springer, Berlin, 1999).
[2] G. Coletti et al., Adv. Funct. Mater. **21**, 879 (2011).
[3] H. Savin, M. Yli-Koski, and A. Haarahiltunen, Appl. Phys. Lett. **95**, 152111 (2009).
[4] S. Esfahani, Thesis Solvent Refining of Metallurgical Grade Silicon Using Iron (Materials Science and Engineering, University of Toronto, 2010).
[5] N. D. Arora, J. R. Hauser, and D. J. Roulston, IEEE Trans. Electron Devices **29**, 292 (1982).
[6] J. Lee and S. R. Morrison, J. Appl. Phys. **64**, 6679 (1988).
[7] T. Buonassisi et al., Patent, Internal gettering by metal alloy clusters, Pub. No.: US 2006/0289091 A1 (2006).
[8] W. Kwapil et al., J. Appl. Phys. **106**, 063530 (2009).
[9] J. Bauer et al., Prog. Photovolt.: Res. Appl. **21**, 1444, (2013).
[10] S. Dubois et al., J. Appl. Phys. **102**, 083525 (2007).
[11] S. Knack, J. Weber, H. Lemke, and H. Riemann, Phys. Rev. B **65**, 165203 (2002).
[12] J. Schmidt and K. Bothe, Phys. Rev. B **69**, 024107 (2004).
[13] J. Junge, A. Herguth, G. Hahn, D. Kreßner-Kiel, and R. Zierer, Energy Procedia **8**, 52 (2011).
[14] J. Lindroos, M. Yli-Koski, A. Haarahiltunen, and H. Savin, Appl. Phys. Lett. **101**, 232108 (2012).
[15] A. Belayachi, T. Heiser, J.P. Schunck, and A. Kempf, Appl. Phys. A **80**, 201 (2005).

